

Methylammonium Tetrel Halide Perovskite Ion pairs and Their Dimers: The Interplay Between the Hydrogen-, Pnictogen- and Tetrel-Bonding Interactions

Pradeep R. Varadwaj^{1,2,*}, Arpita Varadwaj,^{1*} Helder M. Marques², Koichi Yamashita¹

¹ Department of Chemical System Engineering, School of Engineering, The University of Tokyo 7-3-1, Tokyo 113-8656, Japan

² Molecular Sciences Institute, School of Chemistry, University of the Witwatersrand, Johannesburg 2050, South Africa

* Correspondence: pradeep@t.okayama-u.ac.jp (PRV); varadwaj.arpita@gmail.com (A.V.)

Electronic Supplementary Information

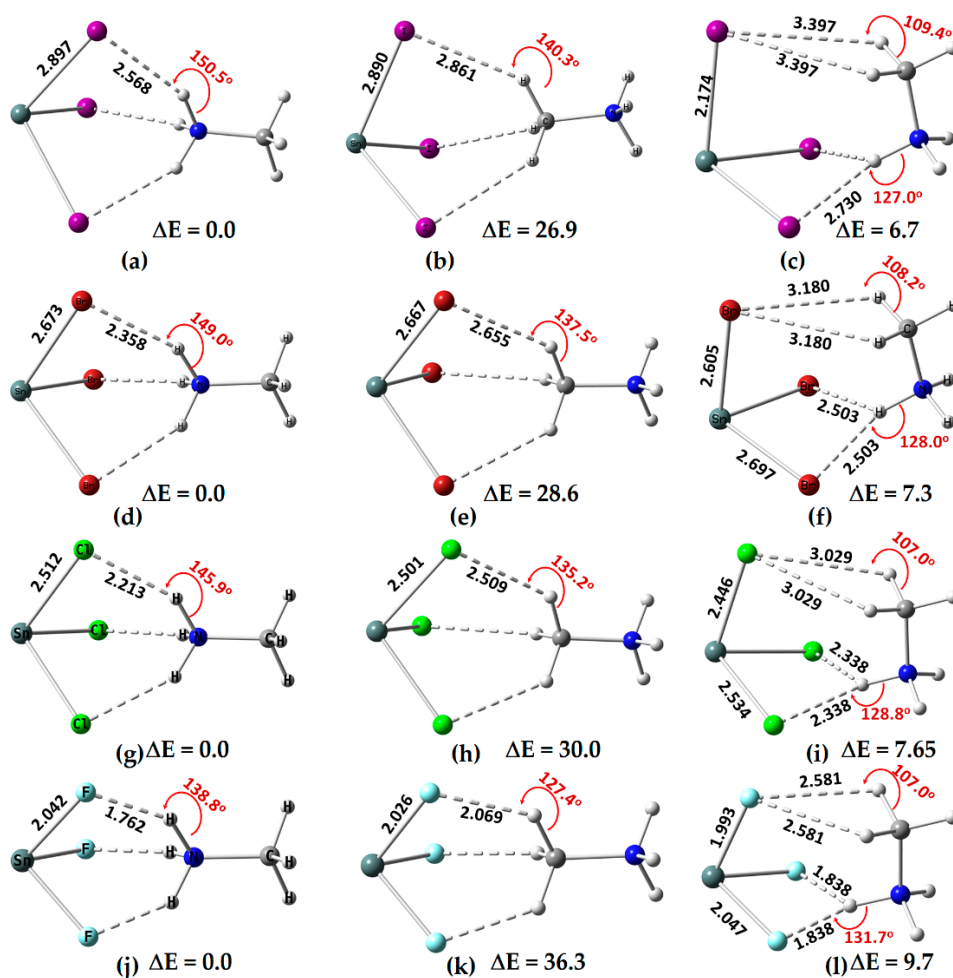


Figure S1. [ω B97XD/def2-TZVPPD] level fully-relaxed geometries of $[\text{CH}_3\text{NH}_3^+\cdot\text{SnX}_3^-]$ ($X = \text{F}, \text{Cl}, \text{Br}, \text{I}$) ion-pairs in the conformational space, including (a) $[\text{I}_3\text{Sn}\cdots\text{NH}_3\text{CH}_3]$; (b)

[I₃Sn...CH₃NH₃]; (c) [Br₃Sn...NH₃CH₃]; (d) [Br₃Sn...CH₃NH₃]; (e) [Cl₃Sn...NH₃CH₃]; (f) [Cl₃Sn...CH₃NH₃]; (g) [Cl₃Sn...H₃NCH₃]. Shown are selected coordinate and hydrogen bond distances in Å and hydrogen bond angles in degrees. The relative energies (ΔE) with respect to the most stable conformer is shown in kcal mol⁻¹. Atom labeling is shown for selected systems.

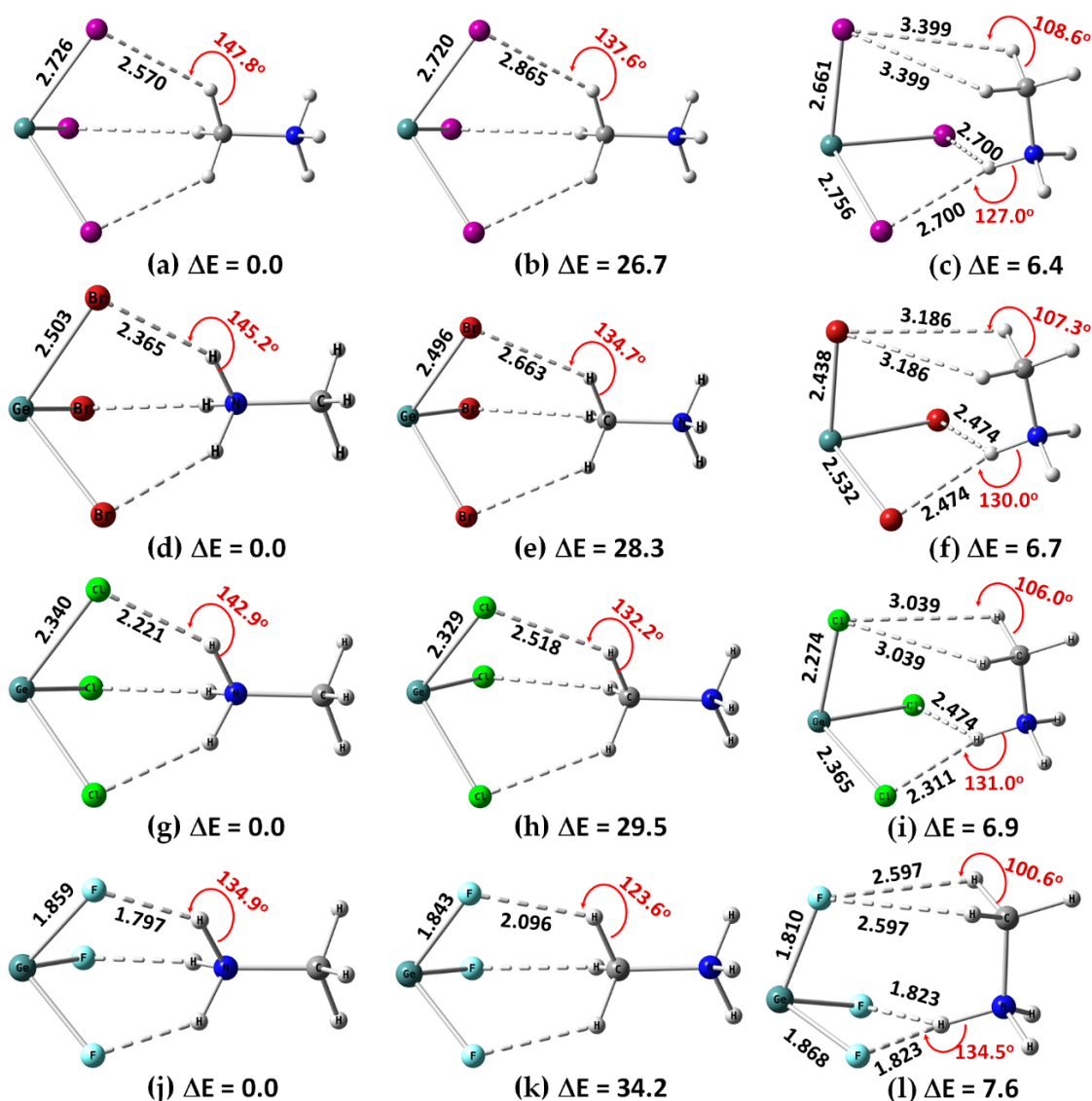


Figure S2. [ω B97XD/def2-TZVPPD] level fully-relaxed geometries of $[\text{CH}_3\text{NH}_3^+\cdot\text{GeX}_3^-]$ ($X = \text{F}, \text{Cl}, \text{Br}, \text{I}$) ion-pairs in the conformational space, including (a) $[\text{I}_3\text{Ge}\cdots\text{NH}_3\text{CH}_3]$; (b) $[\text{I}_3\text{Ge}\cdots\text{CH}_3\text{NH}_3]$; (c) $[\text{Br}_3\text{Ge}\cdots\text{NH}_3\text{CH}_3]$; (d) $[\text{Br}_3\text{Ge}\cdots\text{CH}_3\text{NH}_3]$; (e) $[\text{Cl}_3\text{Ge}\cdots\text{NH}_3\text{CH}_3]$; (f) $[\text{Cl}_3\text{Ge}\cdots\text{CH}_3\text{NH}_3]$; (g) $[\text{Cl}_3\text{Ge}\cdots\text{H}_3\text{NCH}_3]$. Shown are selected coordinate and hydrogen bond distances in Å and hydrogen bond angles in degrees. The relative energies (ΔE) with respect to the most stable conformer is shown in kcal mol⁻¹. Atom labeling is shown for selected systems

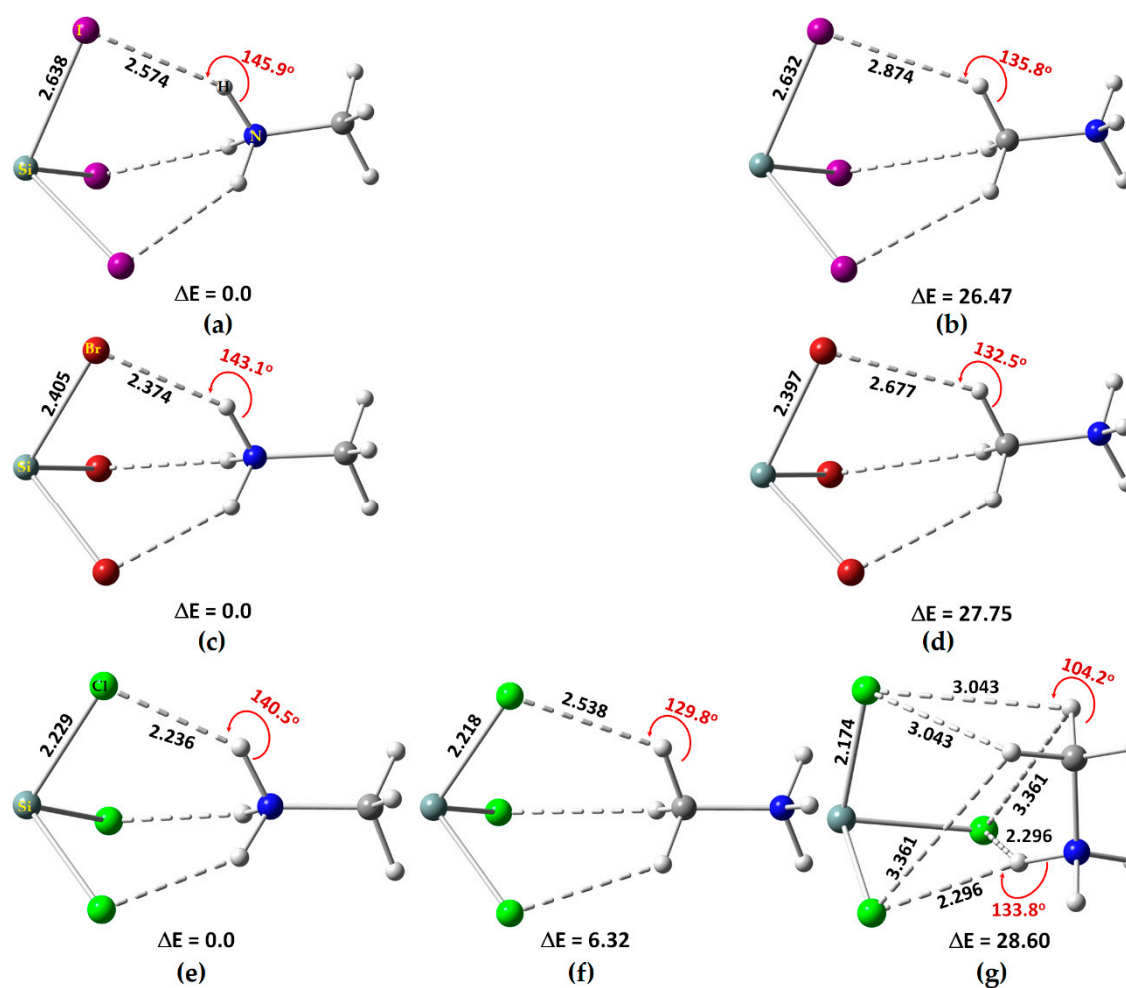


Figure S3. [ω B97XD/def2-TZVPPD] level fully-relaxed geometries of $[\text{CH}_3\text{NH}_3^+ \cdot \text{SiX}_3^-]$ ($X = \text{Cl}, \text{Br}, \text{I}$) ion-pairs in the conformational space, including (a) $[\text{I}_3\text{Si} \cdots \text{NH}_3\text{CH}_3]$; (b) $[\text{I}_3\text{Si} \cdots \text{CH}_3\text{NH}_3]$; (c) $[\text{Br}_3\text{Si} \cdots \text{NH}_3\text{CH}_3]$; (d) $[\text{Br}_3\text{Si} \cdots \text{CH}_3\text{NH}_3]$; (e) $[\text{Cl}_3\text{Si} \cdots \text{NH}_3\text{CH}_3]$; (f) $[\text{Cl}_3\text{Si} \cdots \text{CH}_3\text{NH}_3]$; (g) $[\text{Cl}_3\text{Si} \cdots \text{H}_3\text{NCH}_3]$. Shown are selected coordinate and hydrogen bond distances in Å and hydrogen bond angles in degrees. The relative energies (ΔE) with respect to the most stable conformer is shown in kcal mol⁻¹. Atom labeling is shown for selected systems.

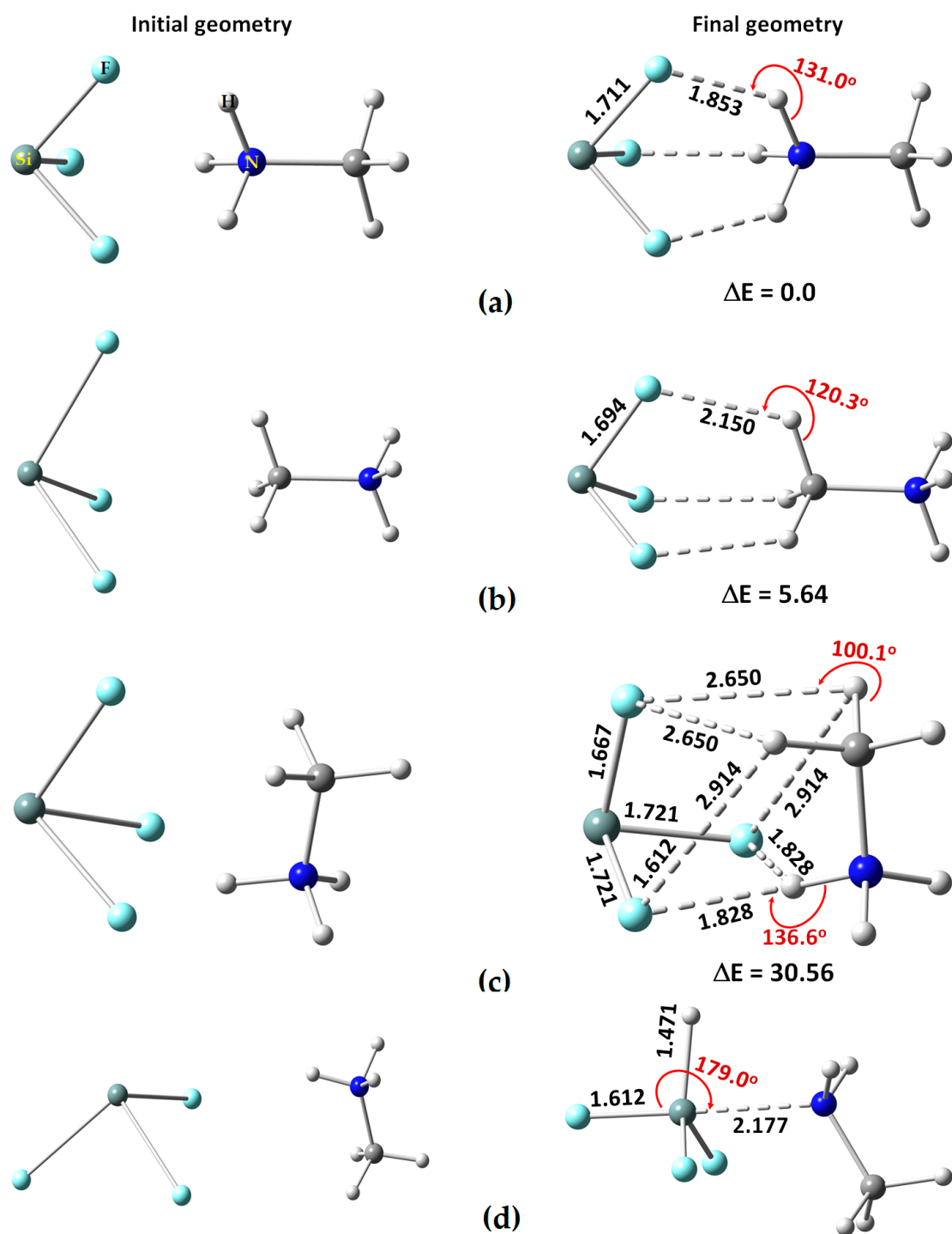


Figure S4. Initial (left) and final [*ω*B97XD/def2-TZVPPD] (right) configurations of $[\text{CH}_3\text{NH}_3^+\cdots\text{SiF}_3^-]$. These include: (a) $[\text{F}_3\text{Si}\cdots\text{NH}_3\text{CH}_3]$; (b) $[\text{F}_3\text{Si}\cdots\text{CH}_3\text{NH}_3]$; (c) $[\text{F}_3\text{Si}\cdots\text{H}_3\text{NCH}_3]$; (d) $\text{F}_3\text{HSi}\cdots\text{NH}_2\text{CH}_3$. Shown (a)-(c) (right) are selected coordinate and hydrogen bond distances in Å and hydrogen bond angles in degrees. The relative energies (ΔE) with respect to the most stable conformer (a) is shown in kcal mol⁻¹. Atom labeling is shown in (a). Shown in (d) are selected coordinate bond and tetrel bond distances in Å and tetrel bond angle in degrees.

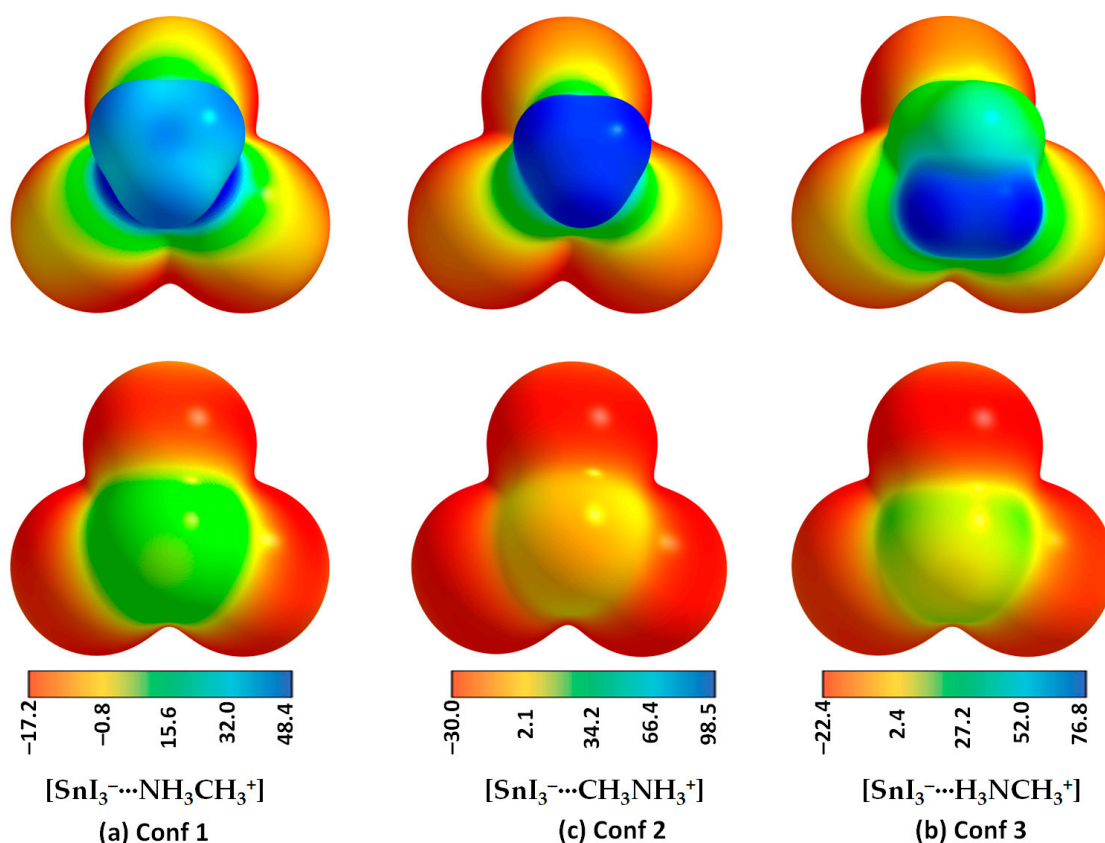


Figure S5. [ω B97XD/def2-TZVPPD] level potential on the electrostatic surface of the three conformations of $[\text{CH}_3\text{NH}_3^+\bullet\text{SnI}_3^-]$: (a) $[\text{SnI}_3^-\cdots\text{NH}_3\text{CH}_3^+]$; (b) $[\text{SnI}_3^-\cdots\text{CH}_3\text{NH}_3^+]$; and (c) $[\text{SnI}_3^-\cdots\text{H}_3\text{NCH}_3^+]$. The methyl, ammonium and both groups of MA are facing the reader in the top panel of (a), (b) and (c), respectively. The Sn atom is facing the reader in the bottom panel of all the three MESP plots shown in (a)-(c). Values on the color bar are in kcal mol^{-1} . Atom labeling is shown for selected systems

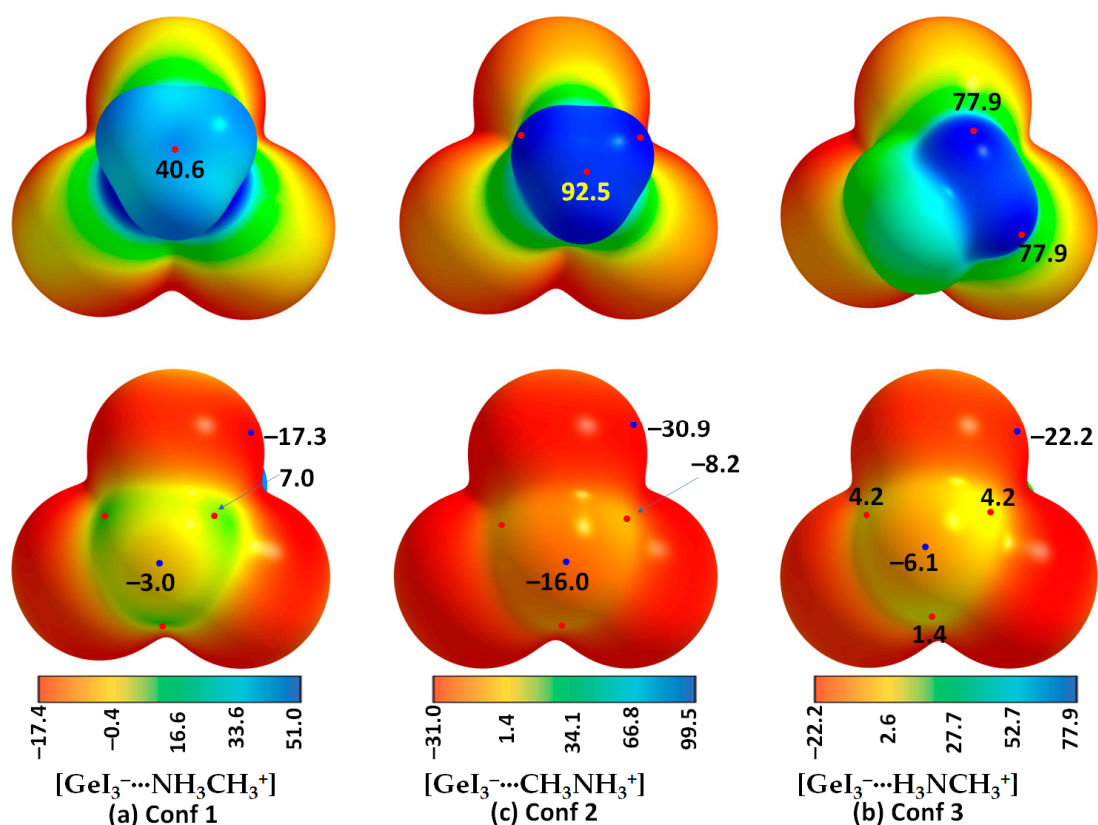


Figure S6. [ω B97XD/def2-TZVPPD] level potential on the electrostatic surface of the three conformations of [CH₃NH₃⁺•GeI₃⁻]: (a) [GeI₃⁻...NH₃CH₃⁺]; (b) [GeI₃⁻...CH₃NH₃⁺]; and (c) [GeI₃⁻...H₃NCH₃⁺]. The methyl, ammonium and both groups of MA are facing the reader in the top panel of (a), (b) and (c), respectively. The Sn atom is facing the reader in the bottom panel of all the three MESP plots shown in (a)-(c). Values on the color bar are in kcal mol⁻¹. Atom labeling is shown for selected systems.

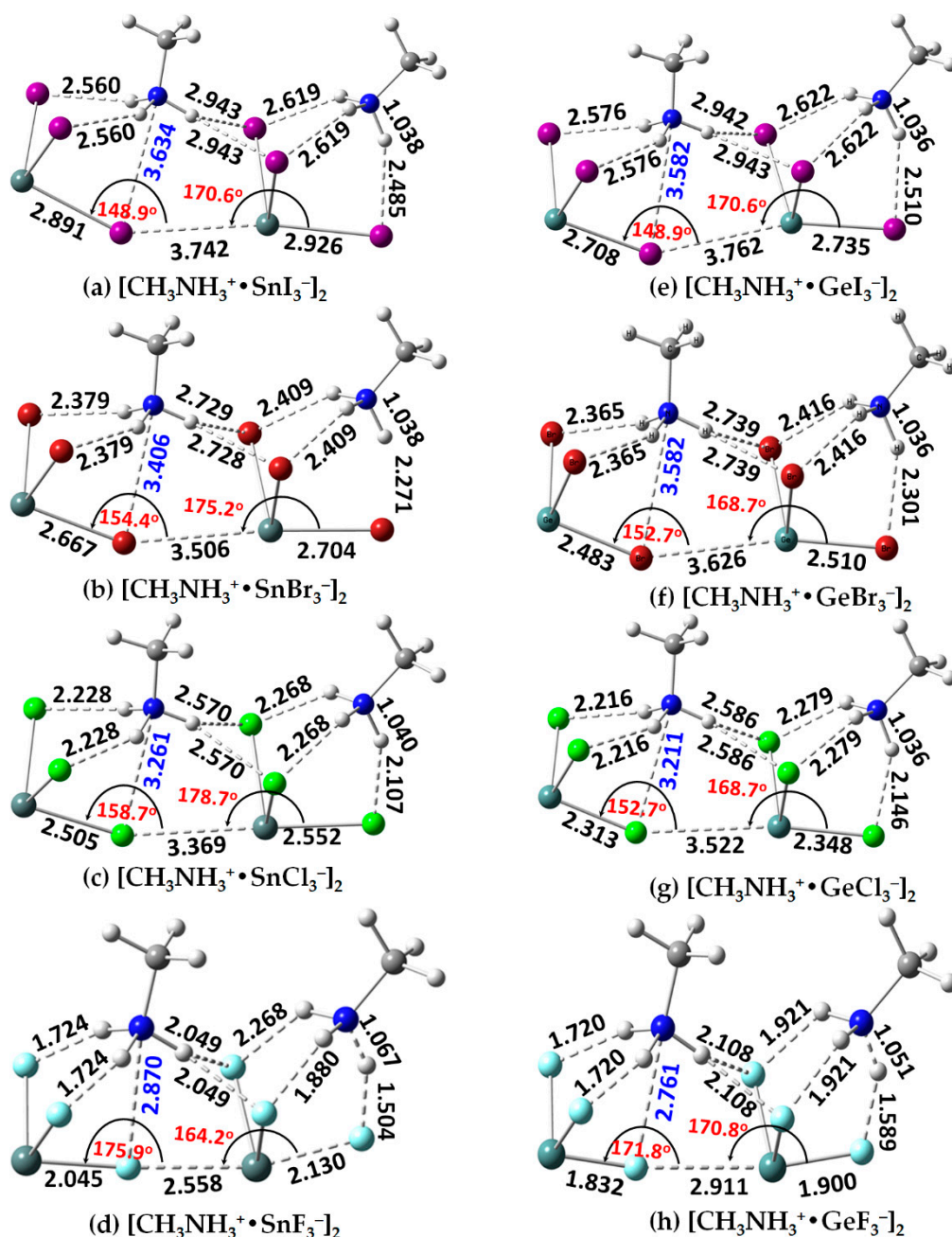


Figure S7. [ω B97XD/def2-TZVPPD] level fully relaxed gas-phase geometries of (a) $[\text{CH}_3\text{NH}_3^+ \cdot \text{SnI}_3^-]_2$; (b) $[\text{CH}_3\text{NH}_3^+ \cdot \text{SnBr}_3^-]_2$; (c) $[\text{CH}_3\text{NH}_3^+ \cdot \text{SnCl}_3^-]_2$; and (d) $[\text{CH}_3\text{NH}_3^+ \cdot \text{SnF}_3^-]_2$; (e) $[\text{CH}_3\text{NH}_3^+ \cdot \text{GeI}_3^-]_2$; (f) $[\text{CH}_3\text{NH}_3^+ \cdot \text{GeBr}_3^-]_2$; (g) $[\text{CH}_3\text{NH}_3^+ \cdot \text{GeCl}_3^-]_2$; and (h) $[\text{CH}_3\text{NH}_3^+ \cdot \text{GeF}_3^-]_2$. Selected bond lengths (\AA) and bond angles (degrees) are shown in (a)-(h).

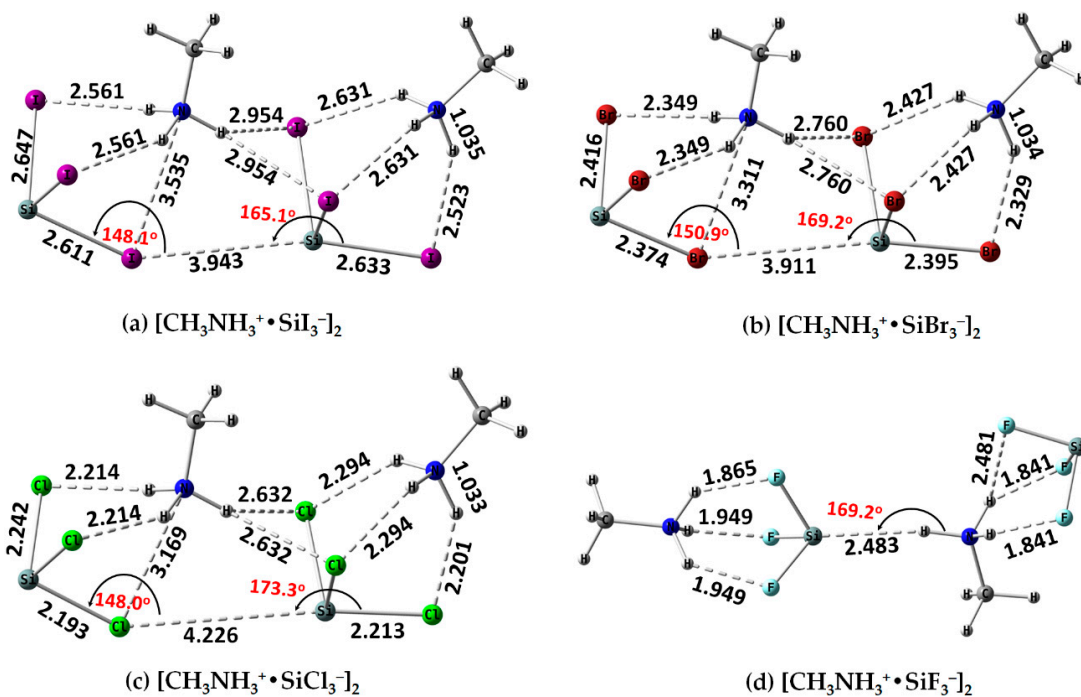
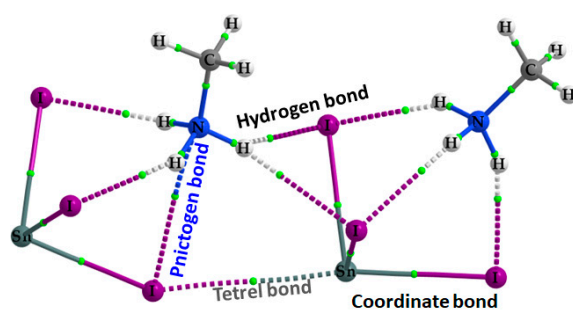
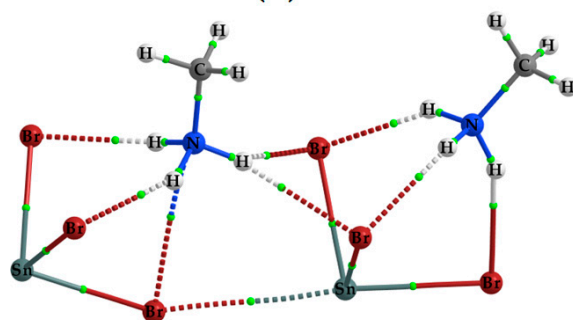


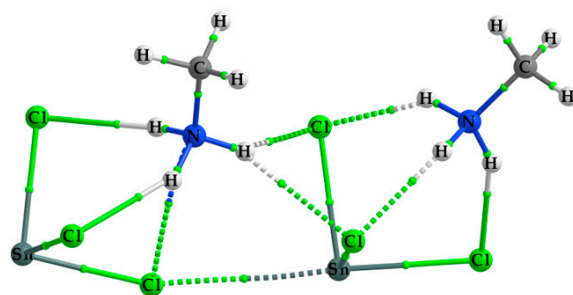
Figure S8. [ω B97XD/def2-TZVPPD] level fully relaxed gas-phase geometries of (a) $[\text{CH}_3\text{NH}_3^+ \cdot \text{SiI}_3^-]_2$; (b) $[\text{CH}_3\text{NH}_3^+ \cdot \text{SiBr}_3^-]_2$; (c) $[\text{CH}_3\text{NH}_3^+ \cdot \text{SiCl}_3^-]_2$; and (d) $[\text{CH}_3\text{NH}_3^+ \cdot \text{SiF}_3^-]_2$. Selected bond lengths (Å) and bond angles (degrees) are shown in (a)-(h). Atom labeling is shown for each case.



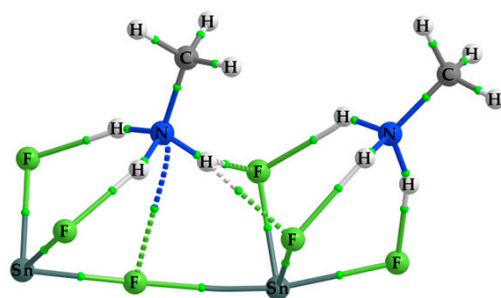
(a)



(b)



(c)



(d)

Figure S9. [ω B97XD/def2-TZVPPD] computed QTAIM based molecular graphs of a) $[\text{CH}_3\text{NH}_3^+\cdot\text{SnI}_3^-]_2$; (b) $[\text{CH}_3\text{NH}_3^+\cdot\text{SnBr}_3^-]_2$; (c) $[\text{CH}_3\text{NH}_3^+\cdot\text{SnCl}_3^-]_2$; and (d) $[\text{CH}_3\text{NH}_3^+\cdot\text{SnF}_3^-]_2$. The bond critical points between atomic basins are shown as tiny spheres in green, and bond paths as solid and lines in atom color. The values (in a.u.) of the charge density (ρ_b), the Laplacian of the charge density ($\nabla^2\rho_b$), and the total energy density (H_b) are given for selected bcps. Bond type and atom labeling is shown

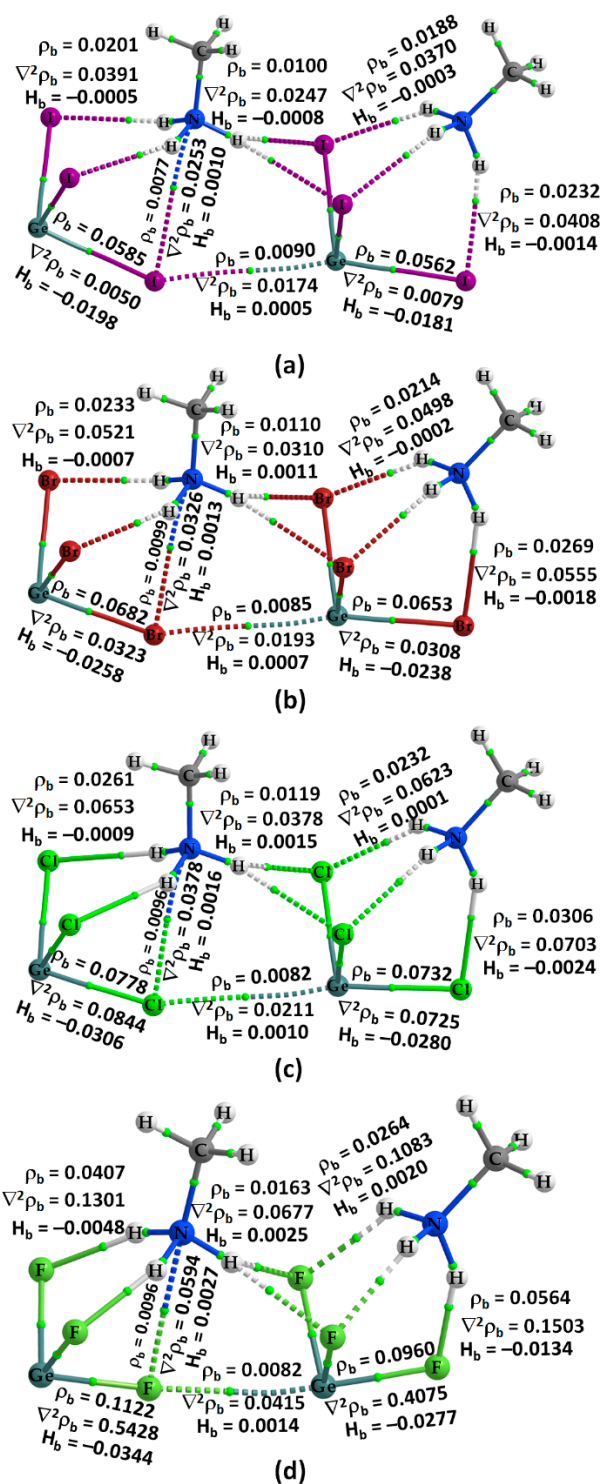


Figure S10. [ω B97XD/def2-TZVPPD] computed QTAIM based molecular graphs of a) $[\text{CH}_3\text{NH}_3^+\bullet\text{GeI}_3^-]_2$; (b) $[\text{CH}_3\text{NH}_3^+\bullet\text{GeBr}_3^-]_2$; (c) $[\text{CH}_3\text{NH}_3^+\bullet\text{GeCl}_3^-]_2$; and (d) $[\text{CH}_3\text{NH}_3^+\bullet\text{GeF}_3^-]_2$. The bond critical points between atomic basins are shown as tiny spheres in green, and bond paths as solid and lines in atom color. The values (in a.u.) of the charge density (ρ_b), the Laplacian of the charge density ($\nabla^2\rho_b$), and the total energy density (H_b) are given for selected bcps. Bond type and atom labeling is shown.

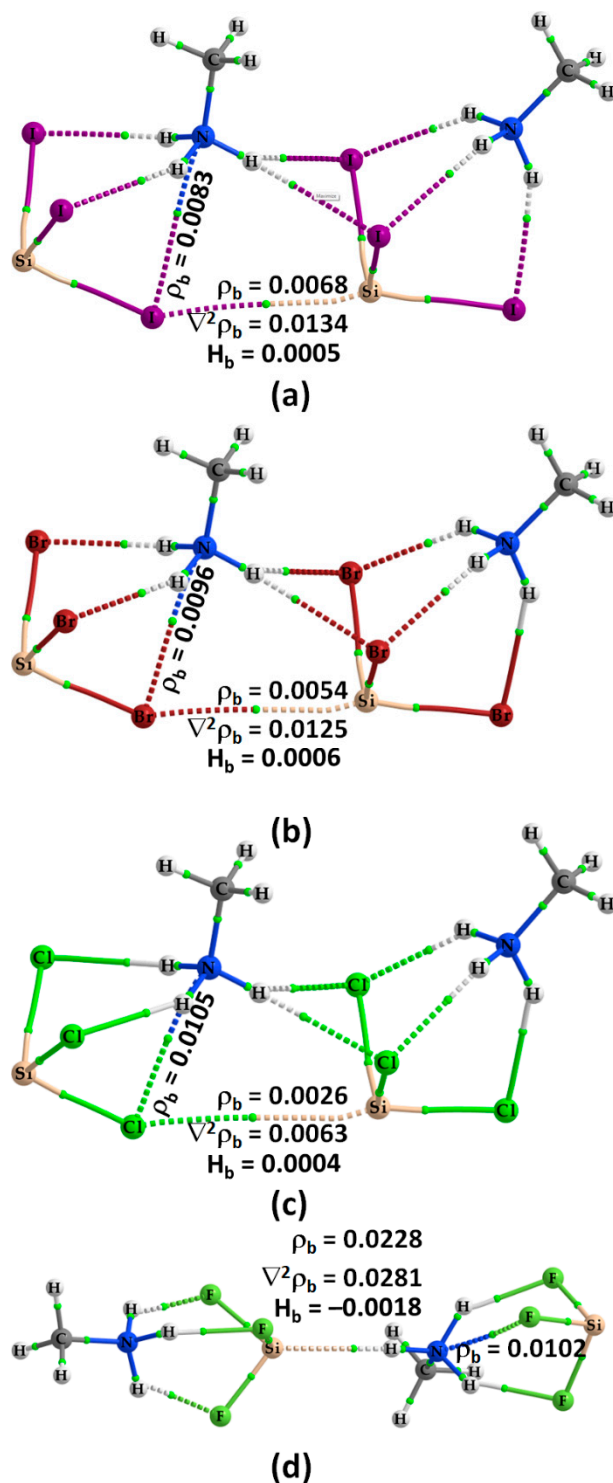


Figure S11. [ω B97XD/def2-TZVPPD] computed QTAIM based molecular graphs of a) $[\text{CH}_3\text{NH}_3^+ \bullet \text{SiI}_3^-]_2$; (b) $[\text{CH}_3\text{NH}_3^+ \bullet \text{SiBr}_3^-]_2$; (c) $[\text{CH}_3\text{NH}_3^+ \bullet \text{SiCl}_3^-]_2$; and (d) $[\text{CH}_3\text{NH}_3^+ \bullet \text{SiF}_3^-]_2$. The bond critical points between atomic basins are shown as tiny spheres in green, and bond paths as solid and lines in atom color. Bond type and atom labeling is shown. Charge density properties (ρ_b , $\nabla^2 \rho_b$, and H_b) in a.u. are shown for selected bcps.

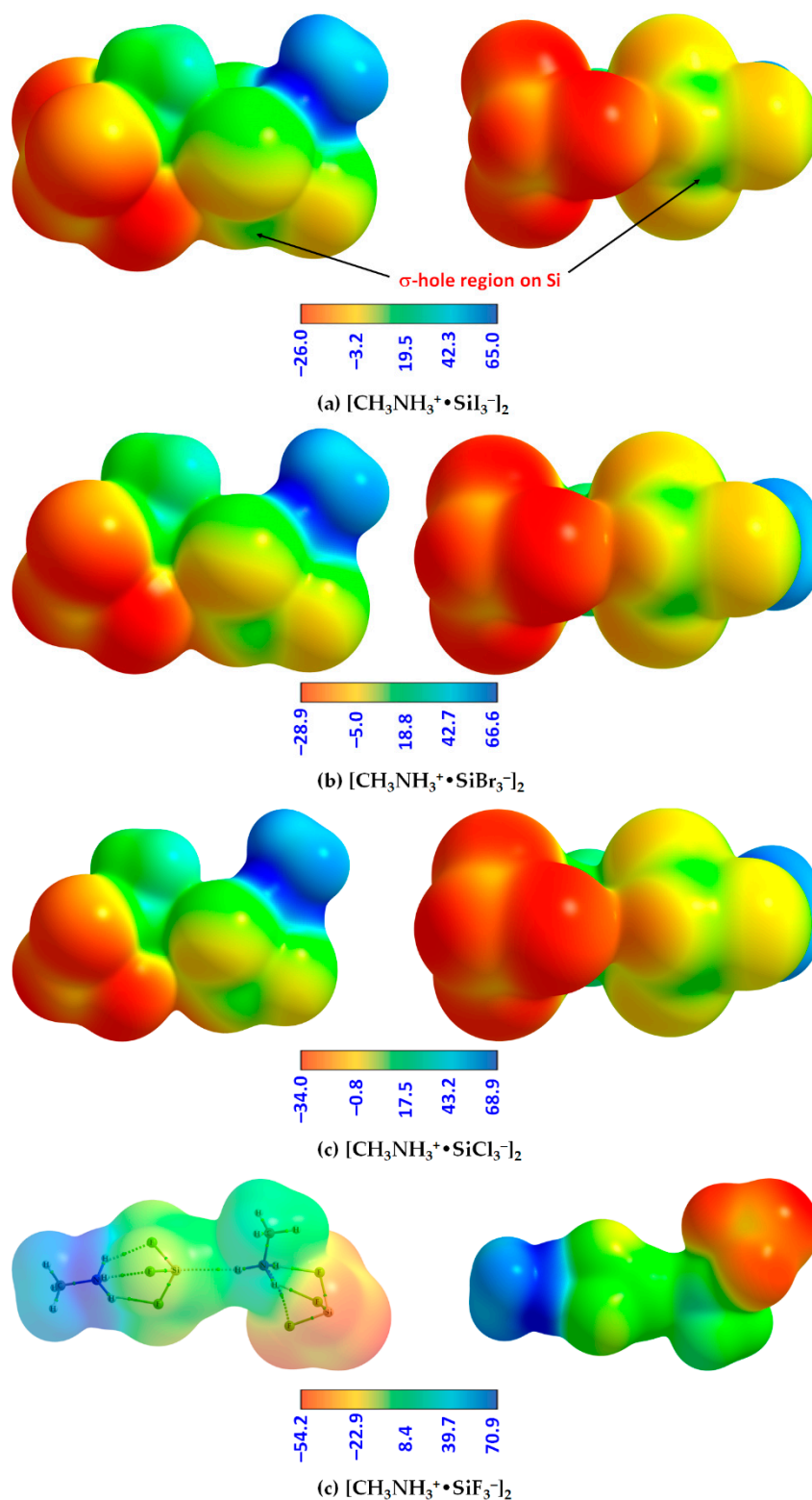


Figure S12. Two different views (left and right) of [ω B97XD/def2-TZVPPD] computed 0.001 a.u. mapped electrostatic potential on the molecular surfaces of a) $[\text{CH}_3\text{NH}_3^+ \cdot \text{SiI}_3^-]_2$; b) $[\text{CH}_3\text{NH}_3^+ \cdot \text{SiBr}_3^-]_2$; c) $[\text{CH}_3\text{NH}_3^+ \cdot \text{SiCl}_3^-]_2$; and d) $[\text{CH}_3\text{NH}_3^+ \cdot \text{SiF}_3^-]_2$. Values on the color bar are in kcal mol⁻¹.

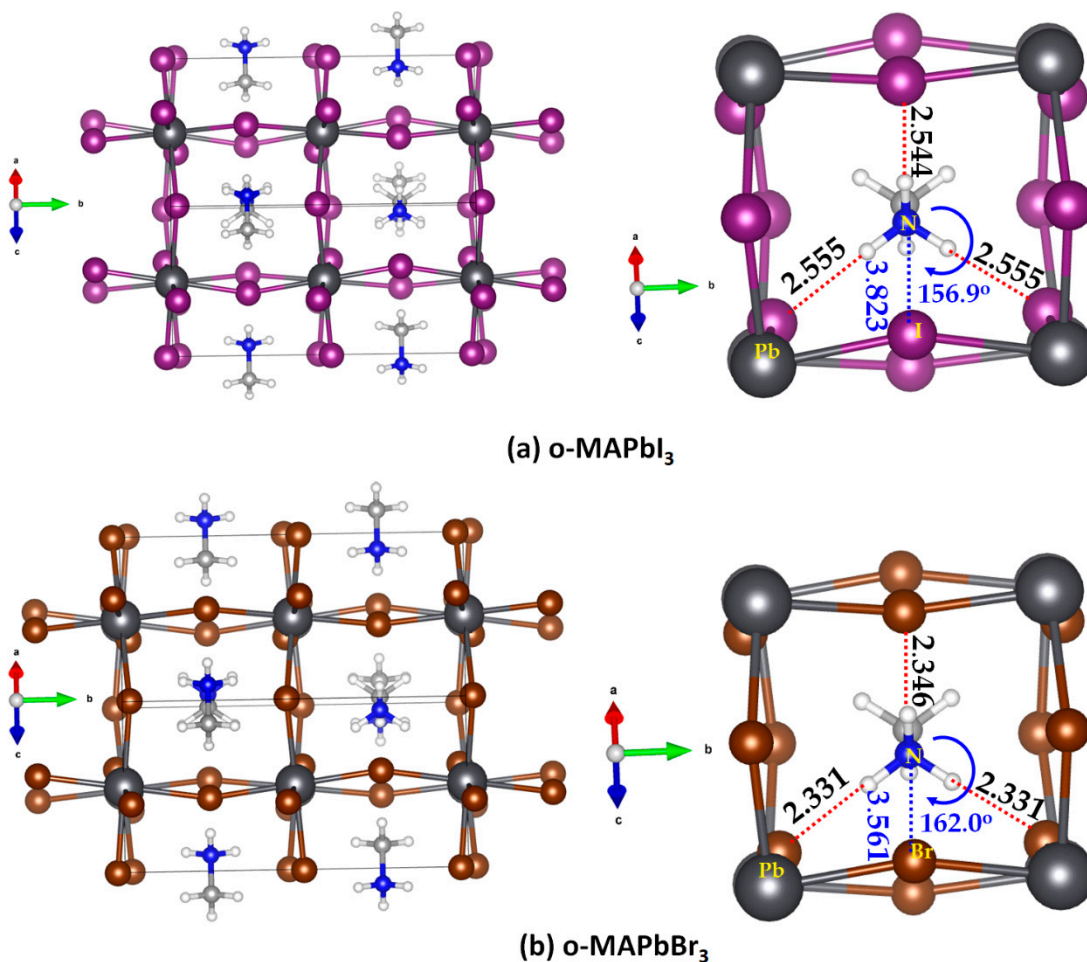


Figure S13. (a) (left) [PBEsol/PAW] relaxed unit-cell geometry of MAPbI₃, showing (right) the nature of N–H···I hydrogen bond and C–N···I pnictogen bond. The pnictogen bond in the crystal (ICSD ref: 428898) of the corresponding has bond distance and bond angle of 3.786 Å and 152.6°, respectively, whereas the three N–H···I hydrogen bonds were 2.807, 2.807 and 2.613 Å. Shown in (b) is the [PBEsol/PAW] relaxed unit-cell geometry of MAPbBr₃, showing (right) the nature of N–H···Br hydrogen bond and C–N···Br pnictogen bond; the bond distance and bond angle of the latter contact in the crystal (ICSD ref: 268782), which has the H atoms in MA missing, were 3.570 Å and 155.0°, respectively. A k-mesh of 4 × 4 × 4, together with the global break condition for the electronic self-consistent and ionic relaxation loops were 10⁻⁶ and -10⁻² eV, respectively, was used. The VASP (version 5.4) code was used.

Table S1. Selected [MP2/def2-TZVPPD] computed 0.001 a.u. isoelectronic density envelope mapped maxima and minima of potential (kcal mol⁻¹) on the electrostatic surfaces of X₃Pb···MA ion-pairs, where X = I, Br, Cl, F, and MA = NH₃CH₃⁺.^a

Ion-pairs	$V_{S,max}(X-Pb)$	$V_{S,max}(X-Pb)$	$V_{S,max}(X-Pb)$	$V_{S,min}(Pb)$	$V_{S,max}(N-C)/V_{S,max}(C-N)$	$V_{S,min}(X)$
I ₃ Pb···NH ₃ CH ₃	25.7	25.7	25.7	23.8	36.2	-17.4
Br ₃ Pb···CH ₃ NH ₃	27.3	27.3	27.3	25.0	35.0	-20.3
Cl ₃ Pb···H ₃ NCH ₃	26.9	26.9	26.9	24.3	33.7	-23.2
F ₃ Pb···NH ₃ CH ₃	24.4	24.4	24.4	19.6	27.0	-37.1

^a The repetition of $V_{S,max}(X-Pb)$ three times suggest that they belong to three equivalent σ -holes along the outer extensions of three Pb-X bonds of the inorganic anion of an ion-pair.

Table S2. Selected [MP2/aug-cc-pVTZ] computed 0.001 a.u. isoelectronic density envelope mapped maxima and minima of potential (kcal mol⁻¹) on the electrostatic surfaces of X₃Pb···MA ion-pairs, where X = I, Br, Cl, F, and MA = NH₃CH₃⁺.^{a,b}

Ion-pairs	$V_{S,max}(X-Pb)$	$V_{S,max}(X-Pb)$	$V_{S,max}(X-Pb)$	$V_{S,min}(Pb)$	$V_{S,max}(N-C)/V_{S,max}(C-N)$	$V_{S,min}(X)$
I ₃ Pb···NH ₃ CH ₃	23.4	23.4	23.4	19.6	36.0	-16.0
Br ₃ Pb···CH ₃ NH ₃	24.5	24.5	24.5	19.7	34.9	-19.1
Cl ₃ Pb···H ₃ NCH ₃	24.3	24.3	24.3	18.8	34.4	-22.4
F ₃ Pb···NH ₃ CH ₃	22.3	22.3	22.3	14.8	27.9	-36.0

^a The pseudo-potential aug-cc-pVTZ-PP was used for Pb and I.

^b The repetition of $V_{S,max}(X-Pb)$ three times suggest that they belong to three equivalent σ -holes along the outer extensions of three Pb-X bonds of the inorganic anion of an ion-pair.